THE SECOND ORDER MANIFOLD METHOD WITH SIX NODE TRIANGLE MESH

Guo-Xin ZHANG[1] , Yasuhito SUGIURA[2], Hiroo HASEGAWA[2] and Guanglun WANG[3]

[1]China institute of Water Resources and Hydropower Research
(Beijing Fuxing-lu A-1, 100038, China)
[2]River Technology Department, I.N.A. Corporation
(Sekiguchi 1-44-10, Bunkyo-ku, Tokyo, 112-8668, Japan)
[3]Professor, Dept. of Hydraulic Engineering, TsingHua University
(Beijing 100084, China)

The manifold method is a recently developed numerical procedure. Based on the original first-order Manifold Method, the second-order one together with corresponding computational code is developed in the present paper. Application examples include calculation of stress distribution of a circular ring, analysis of contact stress of a cylinder compressed between rigid plates, large deformation problem of a cantilever and failure of a slope with discontinuities. The results show that the second-order manifold method is capable in analyzing structure deformation and contact problems with relatively high accuracy and has priority in simulating large deformation problem and failure process.

Key Words: *manifold method, second-order, stress distribution, large deformation, contact, block movement, failure*

1. INTRODUCTION

The discontinuities exist in many engineering structures and foundations. Some of them are settled as need of structure, while others are originated from manufacturing faults or process damages. The occurrence of discontinuities complicates the mechanical feature of structures, burdening the numerical simulation for structure greatly. As we know that the traditional methods in the numerical analysis of discontinuous structures can be classified into two types, one belongs to the category of continuum mechanics, as Finite Element Method (FEM) [1] and Boundary Element Method (BEM) [2]. Some models based on this category of method neglect the existence of individual discontinuity. They treat the structure with joints as continuous media, considering approximately the influence of discontinuities by equivalent model, such as damage tensor, crack tensor or anisotropic element in which the influence of crack distribution is included [3],[4]. Some other models treat the joints by special element such as Goodman Element [5]. This kind of method is used usually in the analysis of deformation or stress of structure before failure. While the second sort belongs to discontinuous analysis method, in which including Discrete Element Method (DEM) [6], Discontinuous Deformation Analysis (DDA) [7] and Rigid Bodies-Spring Model (RBSM) [8]. In this category of methods the structure is treated as dispersed blocks combined by contact units. This method is mainly used in the simulation of structure failure and block movement after failure.

Among these two types, the former one is capable to accurately analyze the deformation and stress distribution inside structure, but has difficulty in simulating discontinuous problem like structure with multi-cracks and block system. The later one can be used to simulate the movement of blocks as well as the contact problem. But it handles one block as one computational element that the stress distribution inside block can not be provided accurately. However, for discontinuous structure with large number of joints the above two traditional methods can not give ideal result.

The Manifold Method (MM) proposed by Shi (1991) [9] combined the advantages of FEM based on the continuum mechanics and DDA based on the discontinuous analytical method together. It has wide applicability in the analysis of stress distribution and block movement after failure. In DDA a sort of effective way in scanning and treating contacts is successfully developed, by which the contact of discontinuities between blocks can be well simulated. The existing limit is that one block is dealt as one computational element. Hence there is no further stress distribution inside block. Under this consideration the MM sets additional mathematical meshes inside blocks to define inner interpolation function, and keeps the computational element in DDA as its physical meshes. As a result the MM is

capable not only in accurately computing stress distribution inside the structure as FEM but also effectively simulating contact of discontinuous and movement of blocks as DDA. Therefore it has wide applicability in the analysis of general structure deformation, large deformation, contact problem and block movement. Its advantage is conspicuous in the simulation of structure with a large number of fractures.

The numerical model of the original MM possess only the first-order accuracy, leading to dissatisfaction in simulating problems that need high accuracy in displacement and stress distribution. Zhang et al.[11] briefly introduced the basic concept of second MM by six node triangle element, in this paper the details of it is proposed. Numerical examples showed the wide applicability of the second-order MM in different field of structure analysis.

2. BASIC CONCEPT OF THE MANIFOLD METHOD

(1) Concept of cover and two sets of meshes

A concept of cover is proposed and two sets of meshes are used in manifold method, indicating differences of MM to FEM. The covers are used to define the local function of each calculation region. One cover covers a fixed region. The shape and size of the region can be freely arranged according to the problem. Covers can be overlapped each other. All covers overlay the whole physical domain.

Two sets of meshes are physical meshes and mathematical meshes. The physical meshes describe the physical domain, which include boundaries, joints and interfaces of blocks. They constitute the integration area. The mathematical meshes, on the other hand, are enclosed lines more or less arbitrarily selected for the definition of covers. The areas enclosed by the mathematical meshes are called mathematical cover, on which the space function is built.

The physical and mathematical meshes intersect each other. If one mathematical cover is divided by a physical mesh into more than one area, each of these areas needs a physical cover.

All of the enclosed areas generated by the intersection of physical meshes with mathematical meshes are defined as calculation elements. Generally the element can be in any shape. One element can be laid over by one or more physical covers. All these physical covers on the element determined its physical behavior. Element is the basic integrate region.

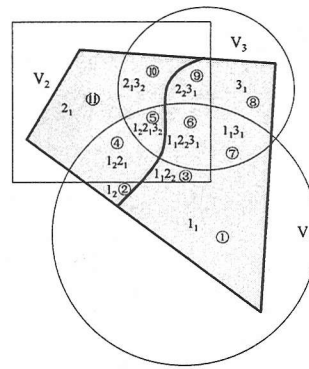**Fig.1**[9] can be used to illustrate the concept of

Fig. 1 General covers and mesh system

cover and meshes introduced above. Thick lines are physical meshes and thin lines are mathematical meshes. Two circles and one rectangle delimit three mathematical covers V_1, V_2 and V_3. The physical meshes divide mathematical cover V_1 into two physical covers 1_1, 1_2, divide V_2 into two physical covers 2_1, 2_2, and divide V3 into two physical covers 3_1, 3_2. Physical meshes intersect with mathematical meshes, forming eleven elements: ①, ②, ③…etc. Physical feature of each element is determined by the physical covers on that element, namely 1_1, 1_2, $1_1 2_2$, $1_2 2_1$, … 2_1 and so on.

Although the mathematical meshes in FEM type MM are the same with the calculation meshes in FEM, the definition of node and element differs from each other. In FEM the node must be placed inside physical domain or at boundary, and the region of element must coincide with interpolation area for interpolation function. While in MM the node can be located outside physical domain, and element region can be detached with interpolation ones. Only one requirement is that the interpolation meshes must cover the entire physical domain. In other words it means that in FEM type MM an element can either be a regular triangle or a part of triangle. In special case when the elements are all identical with the interpolation triangle of mathematical meshes, the calculation grids are exactly the same with that in FEM. In this sense the FEM can be deemed as a special situation of MM. Another difference of FEM with MM is that the element must be regular in FEM while in MM it can be arbitrary, since Simplex Integration[10] is utilized in MM which has no requirement to the shape of element.

(2) Local function and global function

A local function must be defined at every physical cover in MM. Generally the local function can be in any form, as constant, linear function, high-order function, or analytical solution corresponding to physical domain. Combination of

local function by weighting function generates the global function. Suppose a local function at cover U_i is as :

$$u_i(x,y) \qquad (x,y) \in U_i$$

Then global function is obtained by using weight function $w_i(x,y)$ as :

$$u(x,y) = \sum_1^n w_i(x,y) u_i(x,y) \qquad (1)$$

in which :

$$w_i(x,y) \geq 0 \quad (x,y) \in U_i,$$

$$w_i(x,y) = 0 \quad (x,y) \notin U_i , \qquad \sum_{(x,y) \in U_i} w_i = 1$$

Manifold method with FEM mesh usually takes local cover function as constant [9], [11] . Deformation function by constant local function and linear weight function has the same form with that used in three-node triangle element. Local function u_i is unknown variable as in FEM, while weight function $w_i(x,y)$ is the shape function in FEM. Problems like deformation, contact and block movement can be simulated by using this form of local and weighting functions.

3. SECOND-ORDER MANIFOLD METHOD

The second-order MM can be built in either of the following two ways: (1) linear cover function and linear weight function[12]; (2) constant cover function and second-order weight function. The FEM is rich in practices [1], [13] in building displacement function, hence here we follow its course. The mathematical meshes of six-node triangle are shown in **Fig.2**. Second-order displacement function is built by taking constant cover function and second-order weight function. There are two kinds of mathematical covers being used. One is hexagon surrounding all the triangles with a common node, the other is quadrangle surrounding the middle nodes, as shown in **Fig.3**.

(1) Displacement function
The displacement functions take the form of second-order as:

$$u(x,y) = a_1 + b_1 x + c_1 y + d_1 x^2 + e_2 xy + g_1 y^2$$
$$v(x,y) = a'_1 + b'_1 x + c'_1 y + d'_1 x^2 + e'_2 xy + g'_1 y^2 \qquad (2)$$

where $a_1, b_1, c_1 \ldots, a'_1, b'_1, c'_1 \ldots$ are coefficients,

x, y are coordinates inside or on the boundary of the triangle. Suppose the nodal displacement of a basic
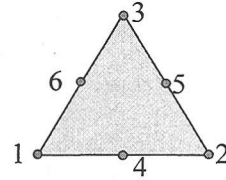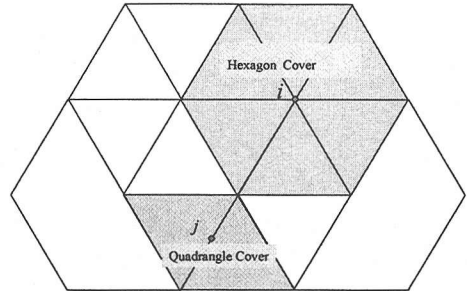

Fig. 2 Six-node basic triangle

Fig. 3 Two types of mathematical covers

triangulate is $\{D\} = \{u_1 \ v_1 \ u_2 \ v_2 \cdots u_6 \ v_6\}^T$, the coefficients in the displacement function (2) can be derived from the nodal coordinates and known displacements of six nodes in mathematical mesh. Substitute the nodal coordinates and displacements into the first formula of equation (2), it can be obtained that:

$$\begin{Bmatrix} u_1 \\ u_2 \\ u_3 \\ \vdots \\ u_5 \\ u_6 \end{Bmatrix} = \begin{bmatrix} 1 & x_1 & y_1 & x_1^2 & x_1 y_1 & y_1^2 \\ 1 & x_2 & y_2 & x_2^2 & x_2 y_2 & y_2^2 \\ \vdots & & & & & \vdots \\ 1 & x_6 & y_6 & x_6^2 & x_6 y_6 & y_6^2 \end{bmatrix} \begin{Bmatrix} a_1 \\ b_1 \\ c_1 \\ d_1 \\ e_1 \\ g_1 \end{Bmatrix}$$

The coefficients in displacement function can be expressed by the nodal coordinate and displacement as:

$$\begin{Bmatrix} a_1 \\ b_1 \\ c_1 \\ d_1 \\ e_1 \\ g_1 \end{Bmatrix} = \begin{bmatrix} 1 & x_1 & y_1 & x_1^2 & x_1 y_1 & y_1^2 \\ 1 & x_2 & y_2 & x_2^2 & x_2 y_2 & y_2^2 \\ \vdots & & & & & \vdots \\ 1 & x_6 & y_6 & x_6^2 & x_6 y_6 & y_6^2 \end{bmatrix}^{-1} \begin{Bmatrix} u_1 \\ u_2 \\ u_3 \\ u_4 \\ u_5 \\ u_6 \end{Bmatrix}$$

taking :

$$\begin{bmatrix} f_{11} & f_{12} & f_{13} & f_{14} & f_{15} & f_{16} \\ f_{21} & f_{22} & f_{23} & f_{24} & f_{25} & f_{26} \\ \vdots & & & & & \vdots \\ f_{61} & f_{62} & f_{63} & f_{64} & f_{65} & f_{66} \end{bmatrix} = \begin{bmatrix} 1 & x_1 & y_1 & x_1^2 & x_1 y_1 & y_1^2 \\ 1 & x_2 & y_2 & x_2^2 & x_2 y_2 & y_2^2 \\ \vdots & & & & & \vdots \\ 1 & x_6 & y_6 & x_6^2 & x_6 y_6 & y_6^2 \end{bmatrix}^{-1}$$

(3)

weight function $w_i(x, y)$ is expressed as : (3)

$$(w_1 \ w_2 \cdots w_6) =$$

$$(1 \ x \ y \ xy \ x^2 \ xy \ y^2) \begin{bmatrix} f_{11} & f_{12} & f_{13} & f_{14} & f_{15} & f_{16} \\ f_{21} & f_{22} & f_{23} & f_{24} & f_{25} & f_{26} \\ \vdots & & & & & \vdots \\ f_{61} & f_{62} & f_{63} & f_{64} & f_{65} & f_{66} \end{bmatrix}$$

(4)

where $w_i = w_i(x, y)$. It can be proved that the coefficients in the two formulae of equation (2) take the same values. Displacement of element yield:

$$\begin{Bmatrix} u(x,y) \\ v(x,y) \end{Bmatrix} = [T(x,y)]\{\delta\}$$

$$= \begin{bmatrix} w_1 & 0 & w_2 & 0 & \cdots & w_6 & 0 \\ 0 & w_1 & 0 & w_2 & \cdots & 0 & w_6 \end{bmatrix} \begin{Bmatrix} u_1 \\ v_1 \\ u_2 \\ v_2 \\ \vdots \\ u_6 \\ v_6 \end{Bmatrix}^e$$

(5)

where, $[T(x,y)]$ is the weight function, which is coincident with the shape function in FEM. The formed displacement function by the way above satisfies the three convergence criteria, namely: ① Rigid displacement is included in displacement function and rigid displacement does not cause strain. ②Constant strain is included in the displacement function. ③ The continuity can be ensured in element and between the adjacent elements within the same path-connected region.

(2) Simultaneous equilibrium equation

Governing equation in MM for dynamic problem takes the form as:

$$[M]\{\ddot{\delta}\} + [C]\{\dot{\delta}\} + [K]\{\Delta\delta\} = \{\Delta F\}$$

(6)

where $[M]$ is mass matrix, $[C]$ is damping matrix, $\{\Delta\delta\}$ is displacement increment, $\{\dot{\delta}\}, \{\ddot{\delta}\}$ are

velocity and acceleration, respectively.

$$[K] = [K_e] + [K_{cn}] + [K_{cs}] + [K_f]$$

where $[K_e]$ is stiffness matrices, $[K_{cn}]$, $[K_{cs}]$ are contact matrixes between blocks and discontinuities. $[K_f]$ is fixed point matrix.

$$\{\Delta F\} = \{F_p\} + \{F_b\} + \{F_f\} - \{F_0\} + \{F_{cn}\} + \{F_{cs}\} + \{F_{fr}\}$$

where $[\Delta F]$ is the total load increment, $\{F_p\}$ is load increment, $\{F_b\}$ is volume force vector, $\{F_f\}$ is equivalent load vector caused by known displacement restriction. $\{F_0\}$ is initial force vector, $\{F_{cn}\}$, $\{F_{cs}\}$ are equivalent load vectors by normal and shear contact. $\{F_{fr}\}$ is equivalent load vector by fiction on contact.

All the matrices can be calculated as below:

(a) Stiffness matrix:

$$[K^e] = \iint_{S_e} [\mathbf{B}]^T [D][B] dx dy$$

(7)

where $[B]$ is the strain matrix and $[D]$ is the elastic matrix.

(b) Mass metrix:

$$[M^e] = \iint_{S_e} \rho [T]^T [T] dx dy$$

(8)

where ρ is unit mass of material.

(c) Initial force matrix :

$$\{F_0\}^e = \iint_{S_e} [B]^T \{\sigma_0\} dx dy$$

(9)

where $\{\sigma_0\}^e$ is the initial stress vector.

(d) Volume force matrix :

$$\{F_b\} = \iint_{S_e} [T]^T \begin{Bmatrix} f_x \\ f_y \end{Bmatrix} dx dy$$

(10)

where f_x, f_y are the unit volume forces of element in x and y direction.
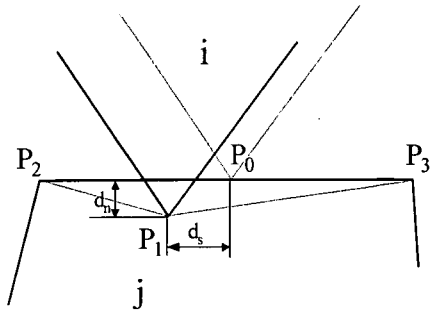
Fig 4 Simulation of contact

(e) Point force matrix:

The load matrix caused by point force is:

$$\{F_p\}^i = [T_i(x_p, y_p)]^T \begin{Bmatrix} P_x \\ P_y \end{Bmatrix} \tag{11}$$

where p_x, p_y are point forces acting at point (x_p, y_p), i is the element at which the point force is acting.

(f) Fixed point matrix:

$$[K^r{}_f] = p[T_r(x_0, y_0)]^T [T_r(x_0, y_0)]$$
$$[F^r{}_f] = -\begin{Bmatrix} pu(x_0, y_0) \\ pv(x_0, y_0) \end{Bmatrix} \tag{12}$$

where x_0 and y_0 are the coordinates of the fixed point, p is the stiffness of the spring addes at the fixed point.

(g) Normal contact matrix:

$$[K_{cn}] = \begin{bmatrix} [K^{cn}{}_{ii}] & [K^{cn}{}_{ij}] \\ [K^{cn}{}_{ji}] & [K^{cn}{}_{jj}] \end{bmatrix}$$

$$[K^{cn}{}_{ii}] = p\{H_i\}\{H_i\}^T, [K^{cn}{}_{ij}] = p\{H_i\}\{G_j\}^T$$

$$[K^{cn}{}_{ji}] = p\{G_j\}\{H_i\}^T, [K^{cn}{}_{jj}] = p\{G_j\}\{G_j\}^T \tag{13}$$

$$[F_i^{cn}] = -p\left(\frac{S_0}{l}\right)\{H_i\}, [F_j^{cn}] = -p\left(\frac{S_0}{l}\right)\{G_j\}$$

where x_1, y_1 are the coordinates of the contact point, and x_2, y_2, x_3, y_3 are the coordinates of the contact line (See **Fig.4**). p is stiffness of contact spring. $l, S_0, \{H_i\}$ and $\{G_i\}$ can be calculated by the

formula as below:

$$l = \sqrt{(x_2 - x_3)^2 + (y_2 - y_3)^2},$$

$$S_0 = \begin{vmatrix} 1 & x_1 & y_1 \\ 1 & x_2 & y_2 \\ 1 & x_3 & y_3 \end{vmatrix}, \quad \{H_i\} = \frac{1}{l}[T_i(x_1, y_1)]^T \begin{Bmatrix} y_2 - y_3 \\ x_3 - x_2 \end{Bmatrix}$$

$$\{G_j\} = \frac{1}{l}[T_j(x_2, y_2)]^T \begin{Bmatrix} y_3 - y_1 \\ x_1 - x_3 \end{Bmatrix} + \frac{1}{l}[T_j(x_3, y_3)]^T \begin{Bmatrix} y_1 - y_2 \\ x_2 - x_1 \end{Bmatrix}$$

where $[T_i(x, y)]$ is the weight function and can be referred to formula (3) to (5).

(h) Shear contact matrix:

The shear contact matrix can be also be calculated by formula (13), but $S_0, \{H_i\}$ and $\{G_j\}$ should be calculated as below:

$$S_0 = (x_1 - x_0 \quad y_1 - y_0) \begin{Bmatrix} x_3 - x_2 \\ y_3 - y_2 \end{Bmatrix}$$

$$\{H_i\} = \frac{1}{l}[T_i(x_1, y_1)]^T \begin{Bmatrix} x_3 - x_2 \\ y_3 - y_2 \end{Bmatrix},$$

$$\{G_j\} = \frac{1}{l}[T_j(x_0, y_0)]^T \begin{Bmatrix} x_2 - x_3 \\ y_2 - y_3 \end{Bmatrix}$$

where x_0 and y_0 are the coordinates of the contact point P_1 on contact line P_2P_3.

(i) Friction force matrix

When the contact point P_1 slides on line P_2P_3, the friction loads should be added to two contacted elements:

$$\{F_i^{fr}\} = \frac{f}{l}[N_i(x_1, y_1)]^T \begin{Bmatrix} x_3 - x_2 \\ y_3 - y_2 \end{Bmatrix}$$

$$\{F_j^{fr}\} = -\frac{f}{l}[N_j(x_0, y_0)]^T \begin{Bmatrix} x_3 - x_2 \\ y_3 - y_2 \end{Bmatrix} \tag{14}$$

where f is the friction force calculated by $f = p \cdot d \cdot \text{sgn} \cdot \tan(\phi)$, ϕ is the friction angle, d_n is penetration depth showed in **Fig. 3**. sgn is the sign of friction force, determined by the angle between P_0P_1 and P_2P_3. It is positive when the angle is smaller than 90° and negative when the angle is more than 90°.
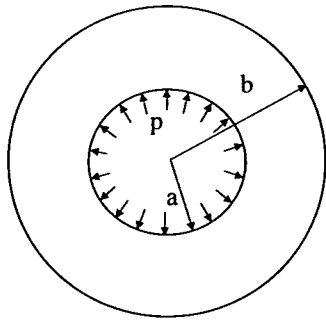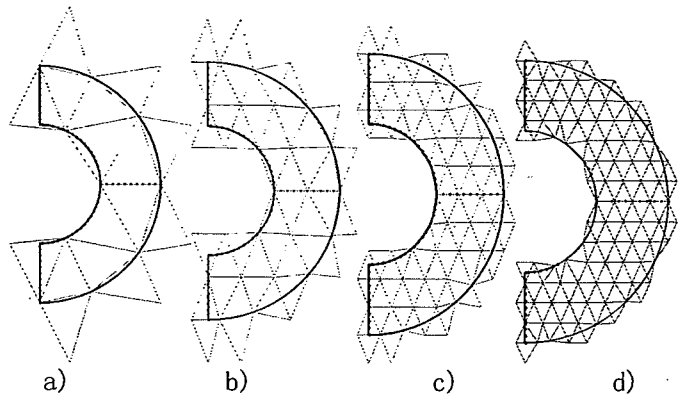
Fig. 5 Circular ring under inner pressure   Fig. 6 Different meshes in computation
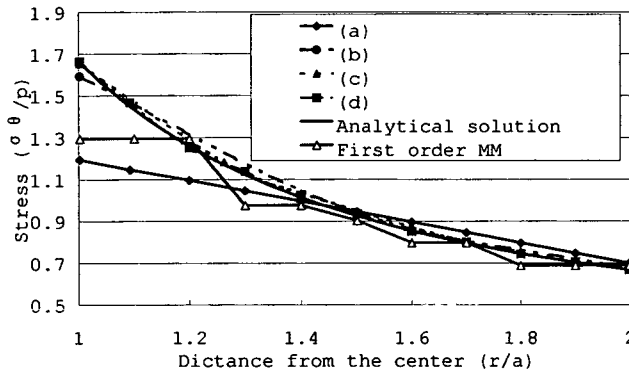

Fig. 7 Comparison of stress distribution

4. NUMERICAL EXAMPLES

(1) General stress and deformation problem

Fig.5 shows a circular ring of inner diameter a and outer diameter b under inner pressure p. Numerical simulations for half of the ring by taking different size of elements (Fig.6) are made, and the results are compared with these of analytical one and the first order MM. The dots in the figure indicate the points of measuring stress. The example is used to check the convergence of the second-order MM. The circumferential stress σ_θ of analytical solution of the problem is[14] :

$$\sigma_\theta = p\frac{(b^2/r^2)+1}{(b^2/a^2)-1}$$

Fig.7 compared the stress distribution of σ_θ along radius. It is shown that the calculation result of the second order MM approaches to the analytical solution gradually as the number of element increases. The result of the first order MM with mesh d) is also given

in this figure It can be seen that the second order MM has a much higher accuracy than the first order MM.

(2) Contact problem

An important application of the second order MM is for the analysis of contact problem. Fig.8 is an example of a cylinder deformation by contact pressure of two rigid plates. The cylinder's radius is 1m. The bottom plate is fixed. The top plate moves downwards in uniform velocity under pressure. The load velocity is 1cm/s. The result of cylinder deformation at different stage of loading is shown in Fig.8(b). Table 1 lists the parameters used in the computation.

Fig.9 gives the contact stress distribution at different loading stages, compared with the solution by Hertz [15] when the displacement of the top plate reaches 0.4m. The comparison shows good agreement between MM solution with Hertz's analysis. Calculated stress curve is not as smooth as analytical one, especially at low load stage. It is caused partly from the simplification of circular section with polygon which is not smooth at its boundary, and partly as the stress on interface of two elements is discontinuous, which is similar to FEM.
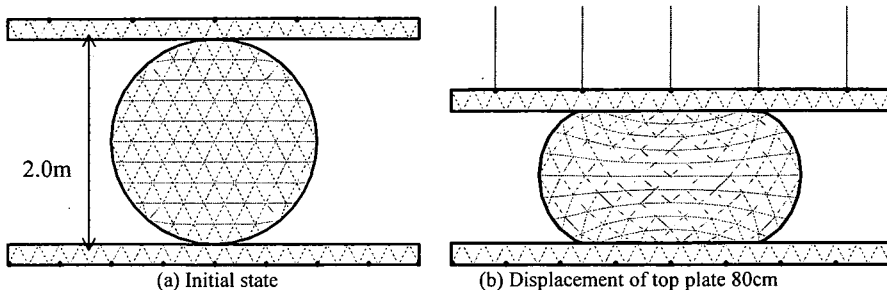
| | (a) Initial state | (b) Displacement of top plate 80cm |

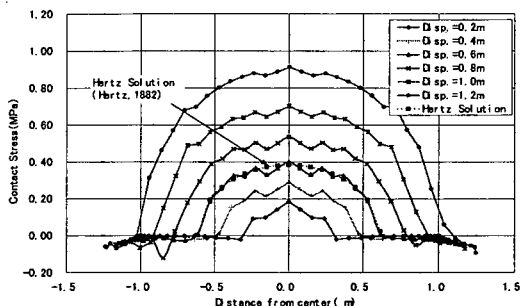**Fig.8** Cylinder deformation by pressure of rigid plates

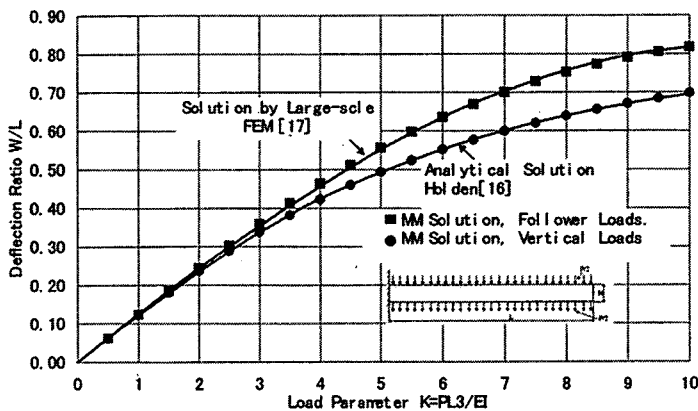**Fig. 9** Contact stress distribution at different deformation stage

Fig. 10 Comparison of large deflection analysis of cantilever under uniformly distributed load

Table 1 Computation parameters

	Elastic module (MPa)	Poisson ratio	Stiffness of contact spring (t/m)
Plates	1000	0.25	200000
Cylinder	1	0.25	200000

(3) Large deformation problem

Equation (6) was solved by step-by-step iteration method. At each computation step a maximum displacement is restricted in order to satisfy small displacement principle. After one step of calculation the computed displacement is added to nodal coordinate, generating new nodal coordinate after deformation. By this way the large deformation is accumulated by small deformation of each step, making MM applicable in simulating the large deformation problem.

As a computation example of large deformation problem the present paper simulated the deformation of a cantilever under uniformly distributed load, compared with analytical solution and FEM numerical result. **Fig.10** shows a cantilever of length L=10m and width H=1m and the comparison of

(a) Step=0,t=0.0   (b) Step=50, t=0.50s

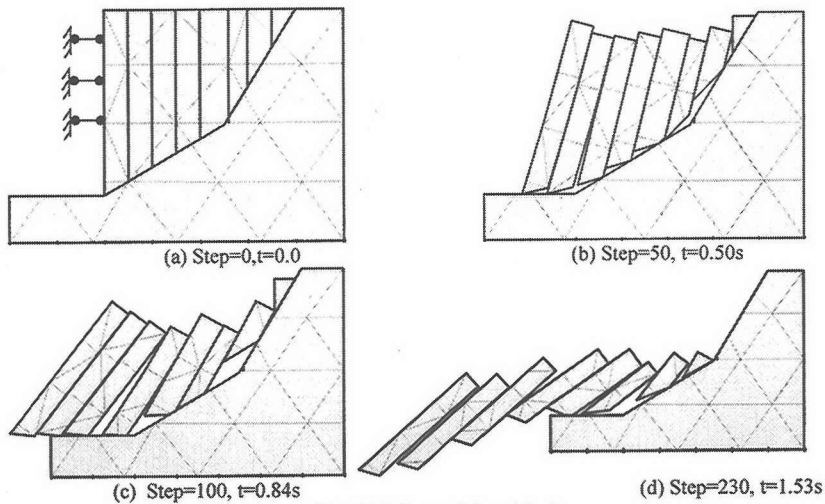(c) Step=100, t=0.84s   (d) Step=230, t=1.53s

Fig. 11 Failure of slope block

deflection at the free end of the cantilever by MM, analytical solution and FEM result[17]. Uniformly distributed load of $P/2$ is loaded on the top and bottom surface of the cantilever. The elastic module E is 120000t/m^2 and Poisson's ratio v is 0.2. Two cases of different load pattern were simulated. (1) Load retains its vertical direction, without change with the beam's deformation. (2) Load keeps its direction perpendicular to the top and bottom surface of the beam, i.e. deformation follower loading. It is seen that an excellent agreement has been obtained with analytical solution reported by Helden and the numerical solution of large deformation FEM.

(4) Block movement problem

By using two sets of meshes and the contact treatment described before, the MM facilitates simulation of deformation and movement problem of block system. A computation example of block sliding failure along slope is given as shown in **Fig. 11**. Gravity is the only load. Computation parameters are: unit gravity ρ =2.5T/m^3 , elastic module E=1000MPa , Poisson's ratio v=0.2 , Penalty p=1000000t/m , maximum calculation time step Δt=0.01s. The blocks are restricted by the left wall initially. At time t=0.0s the restriction is released suddenly, the slope starts sliding under gravity. Slope sliding patterns at different time are shown in **Fig. 11 (b),(c),**and **(d)**. Reasonable results are provided by MM.

5. CONCLUSIONS

The second order manifold method using displacement function and energy principle similar to FEM possesses the same accuracy with FEM. In this paper, the second order displacement function is built by constant cover function and second weight function with six node triangle mathematical mesh, this is the same way with the traditional FEM with triangle mesh. The examples showed that this is a efficient way to built high order manifold method.

The extended MM can not only solve the problem of general structure deformation and stress with relative high accuracy, but also simulate large deformation and contact problem, and especially the structure failure and crack propagation, which require high accuracy in stress and displacement. The extended second order manifold method has the better adaptability in simulating the overall process of structure from deformation to failure and to the movement of failed blocks. Wider application is expected further in the deformation and failure analysis of structure and foundation.

REFERENCES

1) Zienkiewicz, O. C.: *The finite element method in engineering science*, McGraw-Hall, London, 1971.
2) Crouch, S.L. and Starfield, A.M.: 1 *Boundary Element Method in Solid mechanics*, Unwin Hyman Ltd., 1983.
3) Suidan, M.T. and Schonbrich, W.C.: Finite element analysis of reinforced concrete, *J. of the Structural Div. Proc. ASCE*, Vol. 99, No. ST10, pp.2109-2120, 1973.
4) Pande, G.N. et al.: *Numerical Method in Rock Mechanics*, John Wiley & Sons Ltd., 1990.
5) Goodman, R. E. et al.: A model for the mechanics of jointed rock, *J. of Soil Mech. and Foundations Div., Proc. ASCE*, Vol. 94, No. SM3, pp.637-659, 1968.
6) Cundall, P. A.: A computer model for simulating progressive, large scale movements in blocky rock system, ISRM Symposium, Nancy, France, pp.11-18, 1971.
7) Shi, G. H. and Goodman, R. E.: Two-dimensional discontinuous deformation analysis, *Int. Journal Anal. Methods Geomech*, Vol.9, pp.541-556, 1985.

8) Kawai, T.: New element models in discrete structural analysis, *J. of the Society of Naval Architects of Japan*, No. 141, pp.187-193, 1977.

9) Shi, G. H.: Manifold method of material analysis, Trans.9th Arma Conf. On Appl. Math. And Comp., Rep. No.92-1. U.S.Army Res. Office, 1991.

10) Shi, G. H.: Simplex integration for Manifold method, FEM and DDA. Discontinuous Deformation Analysis(DDA) and Simulations of Discontinuous Media.TSI press, pp.205-262, 1996.

11) Zhang, G. X., Sugiura, Y. and Hasegawa, H.: Fracture simulations using manifold and singular boundary element method, *J. of Geotech. Eng. (JSCE)*, No.624/III-47, pp.1-10, 1999.

12) Chen, G. Q., Phnishi, O. and Ito, T.: Development of high order Manifold Method, The Second International Conference on Analysis of Discontinuous Deformation, Kyoto, Japan, pp.132-144, 1997.

13) Rao, S. S.: *The finite element method in engineering*, Pergamon press. 1982.

14) Fung, Y. C.: *Foundation of Solid Mechanics*, Published by Prentice-Hall, Inc. Englewood Cliffs, New Jersy, U. S. A. 1965.

15) Hertz, H.: Uber Die Berugrung fester elastischer Korper, *J. f. d. Reine u. Angewandte Math*. Vol.92, pp.156-171, 1882.

16) Holden, J. T.: On the finite deflections of thin beams, *Int. J. Solids Struc*, Vol.8, pp.1051-1055, 1972.

17) Bathe, K.J., Ramm, E. and Wilson, E. L.: Finite element formulations for large deformation dynamic analysis, *Int. J. Num. Meth. Engng*.,Vol. 9, pp.353-386, 1975.

二次マニフォールド法による変形解析

張国新・杉浦靖人・長谷川浩夫・王光綸

マニフォールド法は近年開発された数値解析法である．本論文は，著者らが発展させた二次マニフォールド法の基本理論を紹介し，応用例として，内圧の作用する円環の応力分布，シリンダーとそれを挟む剛性板の接触応力，片持ち梁の大変形，節理を有する傾斜面の滑り破壊などの解析を行ったものである．その結果，二次マニフォールド法は構造物の変形，接触問題に比較的高い精度を持ち，特に大変形問題や破壊過程のシミュレーションに有効であることが明らかになった．